Catalysis Science & Technology

Broadening the Substrate Range of Serine Palmitoyltransferase by Protein Engineering and Applications to 3-Keto-Dihydrosphingosine Analogs

Journal:	*Catalysis Science & Technology*
Manuscript ID	CY-ART-08-2024-001019.R1
Article Type:	Paper
Date Submitted by the Author:	28-Sep-2024
Complete List of Authors:	Choe, Hyunjun; University of Florida, Department of Chemistry Cha, Minsun; University of Florida, Department of Chemistry Kim, Ahram; University of Florida, Department of Chemistry Stewart, Jon; University of Florida, Department of Chemistry

ARTICLE

Broadening the Substrate Range of Serine Palmitoyltransferase by Protein Engineering and Applications to 3-Keto-Dihydrosphingosine Analogs

Received 00th January 20xx,
Accepted 00th January 20xx

DOI: 10.1039/x0xx00000x

Hyunjun Choe,[a] Minsun Cha, [a] Ahram Kim [a] and Jon D. Stewart *, [a]

Serine palmitoyltransferase produces 3-keto-dihydrosphingosine (KDS) in a single step by a Claisen-like condensation / decarboxylation reaction between L-Ser and palmitoyl-CoA (*n*-C_{16}-CoA). Unfortunately, the enzyme's synthetic potential is limited by its highly restricted substrate range (*n*-C_{14}-CoA to *n*-C_{18}-CoA). We previously reported that the R378K variant of *Sphingomonas paucimobilis* serine palmitoyltransferase (*Sp*SPTase) preferred slightly shorter acyl chain length substrates such as *n*-C_{12}-CoA. While this represented an improvement, we sought to broaden the biocatalyst's substrate range further to allow the synthesis of a much wider range of KDS analogs. Starting from the R378K mutant, we prepared twenty second-generation site-saturation mutant libraries targeting residues lining the active site. Screening with L-Ser and *n*-C_8-CoA as substrates revealed that mutations at only one of the twenty positions yielded improved variants (Tyr 73). Both the acyl-CoA substrate range as well as the interactions with the PLP : L-Ser external aldimine were significantly altered. The best double mutant (R378K / Y73N) showed superior catalytic activity for *n*-C_8-CoA (k_{cat} = 0.44 s^{-1}) while also retaining wild-type thermostability. It even accepted *n*-C_6-CoA and several functionalized acyl-chains, demonstrating the substantially broadened substrate range. Finally, to demonstrate the practical utility of our best variant, we used the R378K / Y73N double mutant to synthesize a short-chain KDS analog on a preparative scale.

Introduction

Serine palmitoyltransferase (SPTase) catalyzes the first step in *de novo* sphingolipid biosynthesis, condensing L-Ser and palmitoyl-CoA (*n*-C_{16}-CoA) to form 3-keto-dihydrosphingosine (KDS) (Figure 1).[1] KDS is subsequently converted to ceramide, the hub of sphingolipid metabolism. Sphingolipids and their associated metabolic pathways have attracted a great deal of attention since they serve vital roles in cell growth, death, senescence, adhesion, migration, inflammation, and intracellular trafficking.[2, 3] Metabolites and enzymes in these pathways are also associated with several pathologies including Alzheimer's and Parkinson's diseases.[4-6] Sphingolipid analogs have therefore been suggested as potential therapeutic agents (Figure 1).[7, 8] Fingolimod (FTY720), a sphingosine analog immunosuppressive drug, was first synthesized in 1992 by modifying the fungal natural product myriocin (ISP-I) and was approved in 2010 by the FDA for treating multiple sclerosis.[9, 10] Cell-permeable, short-chain ceramide analogs (C_2-, C_6-, and C_8-ceramides) have been used to studyceramide-mediated

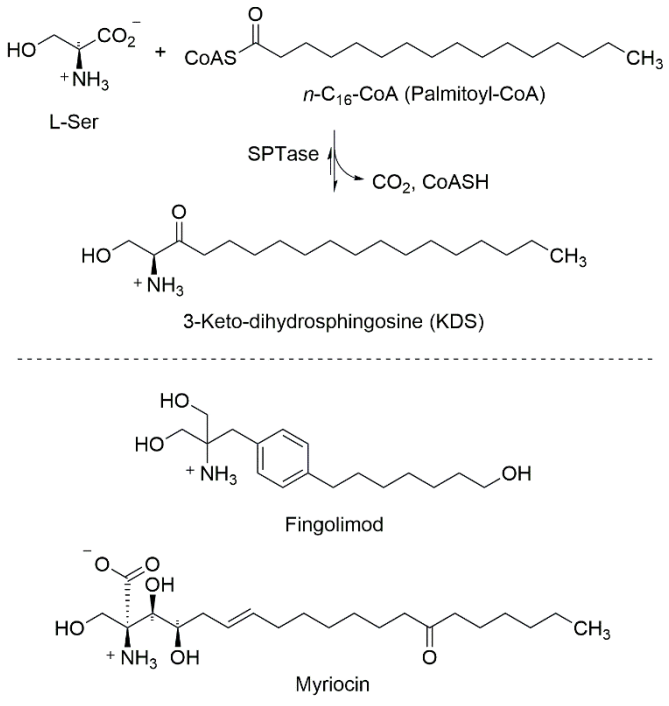

Figure 1. Reaction catalyzed by SPTase and structures of two KDS analogs.

Myriocin

mammalian cell death and its role in neurodegeneration.[11-14] For example, Azuma *et al*. showed that short-chain 3-ketoceramide analogs (C_2-3-ketoceramides) have even stronger

[a] *Department of Chemistry, 126 Sisler Hall, University of Florida, Gainesville, FL 32611 USA. Phone 352.846.0743. E-mail jds2@chem.ufl.edu*

Electronic Supplementary Information (ESI) available: DNA sequence of optimized *Sp*SPTase gene, Lineweaver-Burk plots for acyl-CoA substrates, spectral data for 3-keto-C_{10}-dihydrosphingosine, thioesterase activities for acyl-CoA substrates, overexpression data for R378K / Y73X library members, thermal stabilities of mutants, NMR data for 3-keto-C_8-dihydrosphingosine racemization studies and mutant primers used for libraries. . See DOI: 10.1039/x0xx00000x

apoptosis-inducing activity in human leukemia HL-60 cells than conventionally used C_2-ceramide.[15]

We hypothesized that KDS and its analogs could be synthesized directly by using SPTase to condense L-Ser and the appropriate acyl-CoA. In addition to being efficient, this route would require no protecting groups. SPTase is a member of the α-oxoamine synthase (AOS) family that rely on a pyridoxal 5′-phosphate (PLP) cofactor. For synthetic applications, an SPTase with both high activity and broad substrate tolerance is required. Unfortunately, naturally-occurring SPTases strongly prefer long-chain acyl-CoAs (*n*-C_{16}-CoA and *n*-C_{18}-CoA) and activity drops off dramatically as the length of acyl-chain becomes shorter than 14 carbons.[22] While a viral SPTase does accept a range of acyl-CoAs from *n*-C_4-CoA to *n*-C_{18}-CoA, its extremely low catalytic activity (0.1-11.0 × 10^{-6} U/mg) makes it impractical for preparative use.[23]

We selected the SPTase from *Sphingomonas paucimobilis* (*Sp*SPTase) as the starting point for our synthetic strategy. In addition to its high activity, *Sp*SPTase is soluble (rather than membrane bound), which allows much greater protein overexpression. Its strong preference for long-chain acyl-CoA substrates (*n*-C_{16}-CoA is optimal) is its major deficiency. To help overcome this problem, we developed the R378K variant of *Sp*SPTase that provided higher activities as well as an altered substrate preference that favored somewhat shorter-chain acyl-CoA substrates (*n*-C_{10}-CoA and *n*-C_{12}-CoA).[24] While this was an improvement, the mutant was still incapable of preparing the full range of desirable short-chain KDS analogs needed for sphingolipid studies.

The goal of the present study was to develop *Sp*SPTase variants that would accept an even broader substrate range that encompassed short-chain acyl-CoAs and to demonstrate the utility of this tool by synthesizing an important KDS analog. We applied a semi-rational strategy using site-saturation mutagenesis[25] along with a colorimetric, medium-throughput screening methodology based on Ellman's reagent[26] to twenty active site amino acids. These efforts yielded a significantly improved double mutant (R378K / Y73N) with both a broad substrate range and a preference for shorter-chain acyl-CoAs (*n*-C_6-CoA and *n*-C_8-CoA). This represents a significant alteration in the substrate preference of *Sp*SPTase.

Results and discussion

To develop *Sp*SPTase variants that accepted short, functionalized, and thus more synthetically useful acyl-CoA substrates, we identified twenty residues lining the active site and the alkyl-chain binding tunnel using the crystal structure of the enzyme complexed with product analog decarboxymyriocin (Figure 2A).[35] We applied site saturation mutagenesis to these positions individually in an R378K background and assessed the libraries, seeking double mutants with even greater catalytic activity for short-chain acyl-CoAs as compared to the R378K parent. The starting variant showed 3.8- and 3.2-fold higher activities for *n*-C_{10}-CoA and *n*-C_{12}-CoA, respectively compared to the wild-type but very low activities for < C_{10} acyl substrates.[24]

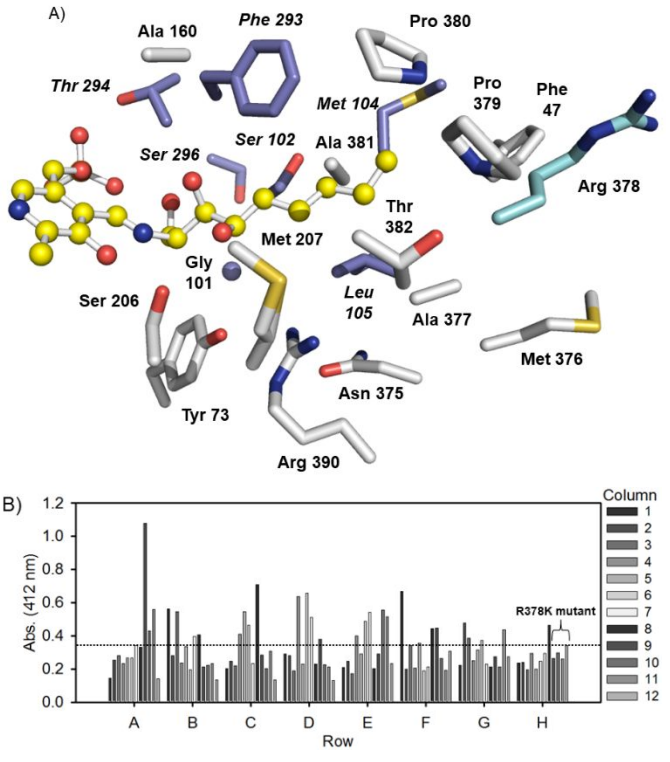

Figure 2. Library construction and screening of SpSPTase double mutant libraries. **Library construction and screening of *Sp*SPTase double mutant libraries.** A) Active site of *Sp*SPTase complexed with PLP : decarboxymyriosin (PDB code 4BMK).[35] Twenty target residues in the active site selected for NNK site-saturation mutagenesis as well as Arg 378 are shown in sticks, and the ligand is shown in ball-and-stick. Residues shown with purple carbons and labels in italics are from the second subunit. B) Screening data from the R378K / Y73X mutant library using L-Ser and *n*-C_8-CoA. Error bars represent differences from duplicate measurements.

We used PCR-based site saturation mutagenesis with an NNK doping scheme for the randomized codon.[25] The native *Sp*SPTase gene contains regions with high GC content (up to 82%), which made PCR amplifications difficult.[24] We therefore used a sequence optimized, synthetic *Sp*SPTase gene with the R378K mutation incorporated as the template for all twenty libraries. The diversity of each library at the randomized codon was assessed by quantitatively analyzing DNA sequencing data as described previously.[25] In all cases, the Q_{pool} scores ranged between 0.79 and 0.93, indicating high quality libraries with very little contamination by artifacts such as primer concatamers, template carryover, etc. Each of the twenty libraries was screened in an individual 96-well plate (*ca*. 3-fold over sampling) with *n*-C_8-CoA as the acyl donor. Ellman's reagent was used to detect free CoASH by-product of the Claisen condensation / decarboxylation reaction.[24]

Of the twenty libraries screened, nineteen showed no significantly improved double mutant variants. By contrast, one quarter of the double mutants in the R378K / Y73X library showed higher absorbance signals than the single mutant parent (R378K) (Figure 2B). This was not a screening artifact since other libraries showed only low levels of free CoASH due to spontaneous thioester hydrolysis and / or *E. coli* thioesterases; rather, one or more replacements for Tyr 73 provided *Sp*SPTase double mutants with higher activities for *n*-

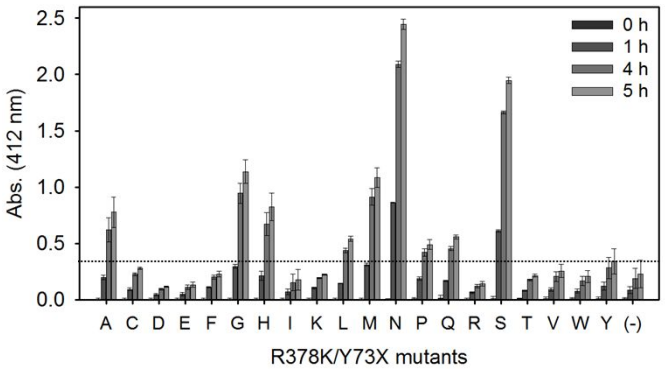

Figure 3. Time course for R378K / Y73X SpSPTase mutants using L-Ser and n-C8-CoA as substrates.

C_8-CoA. Sequencing positives with higher absorbance signals than the starting protein revealed Ala, Gly, Met, Asn, and Ser at position 73. To ensure that all variants at position 73 were tested, each was prepared individually and a time course was measured for each using *n*-C_8-CoA (Figure 3). Although the negative control gave a small signal resulting from self-hydrolysis of *n*-C_8-CoA and esterases and thioesterases present in *E. coli* cell lysates,[36] the background activities were insignificant (0.002 U /mL) for all acyl-CoAs tested (from *n*-C_4-CoA to *n*-C_{16}-CoA) (Figure S5). SDS-PAGE analysis showed that all Tyr 73 variants were overexpressed well and at similar levels in the crude extracts (Figure S6). In addition to the five successful amino acid substitutions detected in the initial library screen (Ala, Gly, Met, Asn, and Ser), the His replacement for Tyr 73 also showed higher activity for *n*-C_8-CoA as compared to the R378K parent.

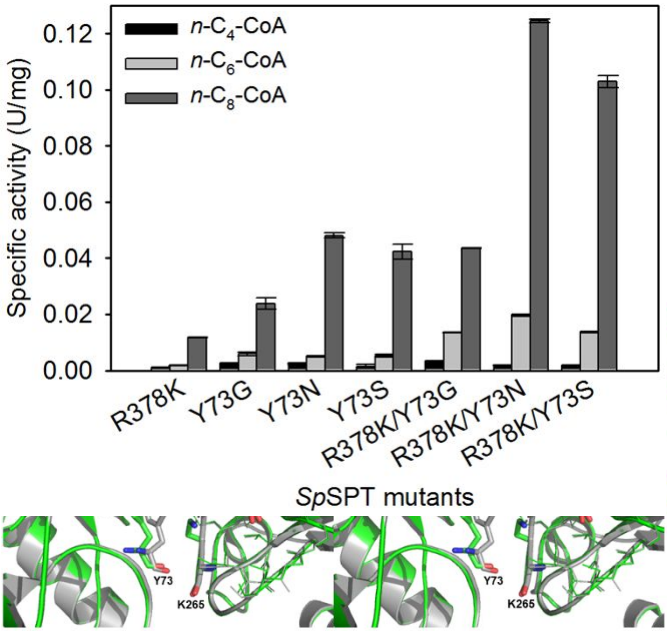

One possible explanation for these results is that a smaller amino acid is required at position 73 for the enzyme to accept shorter acyl-CoAs. Interestingly, Val, Thr, and Asp were not successful replacements for Tyr 73, despite being (apparently) appropriately sized. A closer look, however, reveals that a β-methyl would not fit within the small space (3.6 Å) between the C_β of Tyr 73 and the C_γ of Lys 265 in the PLP : L-Ser external aldimine-bound form (Figure 4). A negative charge at this position might also form strong salt bridges with either the guanidinium group of Arg 390 or the ε-amino group of Lys 265, both catalytically important residues, thereby hampering the catalytic cycle.[37] It was also noteworthy that the R378K / Y73S double mutant showed the second highest activity for *n*-C_8-CoA but the analogous Cys double mutant showed no activity. This might be due to enzyme inactivation by the bulky adduct formed between Ellman's reagent and the Cys thiol moiety.[38] For example, clostridial glutamate dehydrogenase was inactivated by Ellman's reagent (1 : 1 stoichiometry on a subunit basis) due to the presence of the non-catalytic Cys 320 close to the active site. As expected, the C320S mutant was unaffected by Ellman's reagent.[39, 40]

Based on our screening results, the three double mutants with the highest activities were purified and characterized further (R378K / Y73G, R378K / Y73N, and R378K / Y73S). The specific activities of each double mutant for a series of acyl-CoAs (*n*-C_4-CoA to *n*-C_8-CoA) were compared with the corresponding single mutants (R378K, Y37G, Y37N, and Y73S) (Figure 5). The R378K / Y73N double mutant showed the highest activity for *n*-C_8-CoA, which mirrors the result obtained from studies with cell lysates (Figure 3). None of the single mutants showed higher activity than the corresponding double mutants, and the mutations at Arg 378 and Tyr 73 position showed a slight synergistic effect in case of the R378K / Y73N and R378K / Y73S double mutants.

Figure 5. **Specific activities of purified *Sp*SPTase mutants with *n*-acyl-CoAs.**

Figure 4. Stereoview of SpSPTase with the PLP internal aldimine versus the PLP: L-Ser external aldimine. The PLP-bound structure (PDB: 2JG2)41 and the external aldimine-bound structure (PDB: 2W8J)22 are shown in gray and green, respectively. Ligands (PLP and the external aldimine), catalytically important residues (Lys 265, His 159, and Arg 390), Arg 378 on the flexible loop, and Tyr 73 are depicted with sticks. Other residues within 7 Å distance from the external aldimine are shown with lines and polar contacts are shown by dashed lines.

Active site structures of *Sp*SPTase in the absence and presence of the PLP : L-Ser external aldimine are shown in Figure 4.[22, 41] The positions of most residues within 7 Å of the external aldimine were unchanged, but three (Arg 378, Arg 390, and Tyr 73) noticeably reoriented upon external aldimine formation. These changes are likely mechanistically important since enzymes in the AOS family control substrate orientations during catalytic cycles by enzyme conformational changes.[42, 43] Our protein engineering results demonstrated that two of these three residues (Arg 378 and Tyr 73) also play key roles in acyl-substrate preference and can be altered without loss of catalytic activity.[24] The side-chain of Arg 378 plays an important role in the catalytic cycle by stabilizing a quinonoid intermediate[43] and we found that Lys substitution at this non-conserved position altered the substrate preference.[24]

Residues at positions 390 and 73 (*Sp*SPTase numbering) cooperate closely in the catalytic cycle. In AOS family members, Arg is almost universally conserved at position 390 and Asn is the most common residue at position 73, although it is occupied

by Tyr in *Sp*SPTase and some other bacterial SPTases including *S. wittichii* as well as in human SPTases.[44] Ikushiro *et al*. proposed that Arg 390 interacts with the carboxyl group of the external aldimine by hydrogen bonding and ionic interactions, thereby fixing its position so that the H-C_α bond is almost perpendicular to the PLP plane (Dunathan conformation).[37] In addition to interactions with the external aldimine, the side-chain of Arg 390 also interacts with the amino acid at position 73, sometimes with intervening water molecules.[45] For example, in the structure of *Sphingobacterium multivorum* SPTase, Asn 52 interacts indirectly with Arg 367 and the PLP : L-Ser external aldimine *via* water molecules, and both residues are thought to cooperate in fixing the carboxylate of L-Ser during the catalytic cycle.[46] Tyr at position 73 allows direct hydrogen bonding with Arg 390 in the absence of intervening water molecules, as seen in the structures of the bacterial SPTases from *S. paucimobilis* and *S.wittichii*. The precise role of Tyr 73 in *Sp*SPTase remains undefined. It may help fix the location of Arg 390 or it may interact with a quinonoid intermediate by stacking parallel to the plane formed by the guanidinium group of Arg 390 and the carboxyl group of L-Ser.[46] The positions of Arg 390 and Tyr 73 in *Sp*SPTase are nearly the same as those of Arg 390 and Asn 73, respectively, in other AOS family members, suggesting a conserved role in all of these enzymes[47] (Arg 374 and Asn 54 in *Rhodobacter capsulatus* 5-aminolevulinate synthase, ALAS;[48, 49] Arg 361 and Asn 47 in *E. coli* 8-amino-7-oxononanoate synthase, AONS).[45] Based on our results from site-saturation mutagenesis at position 73, a Tyr at this position in *Sp*SPTase is clearly not essential for the catalytic activity. Furthermore, both the wild-type and the R378K / Y73N double mutant are stable at 45 °C, arguing against a major role in stabilizing the enzyme's structure (Figure S7).

Since Tyr 73 in *Sp*SPTase lies near the L-Ser moiety of the external aldimine, we suspected that mutating this residue might also affect L-Ser binding. We measured UV-Vis spectra, which probe several aspects of substrate binding such as the enolimine / ketoenamine tautomeric equilibrium as well as intermediate states during catalytic cycles of PLP-dependent enzymes.[50, 51] Wild-type *Sp*SPTase and the R378K mutant showed little difference in spectral profiles or K_D values for L-Ser (1.4 and 1.2 mM for wild-type and R378K, respectively).[24] By contrast, spectra of the PLP-bound *holo*-forms of the R378K and R378K / Y73N variants were quite different, with shifted λ_{max} values (Figure 6). Absorbance maxima of the enolimine and ketoenamine forms generally appear at 330-340 nm and 410-430 nm, respectively, although alterations in the active site environment can affect these values.[52] The enolimine and ketoenamine λ_{max} values for the internal aldimine state (PLP-bound *holo*-form) of the R378K single mutant were 335 and 425 nm, respectively. By contrast, these peaks were slightly red-shifted in the R378K / Y73N double mutant to 337 and 431 nm.

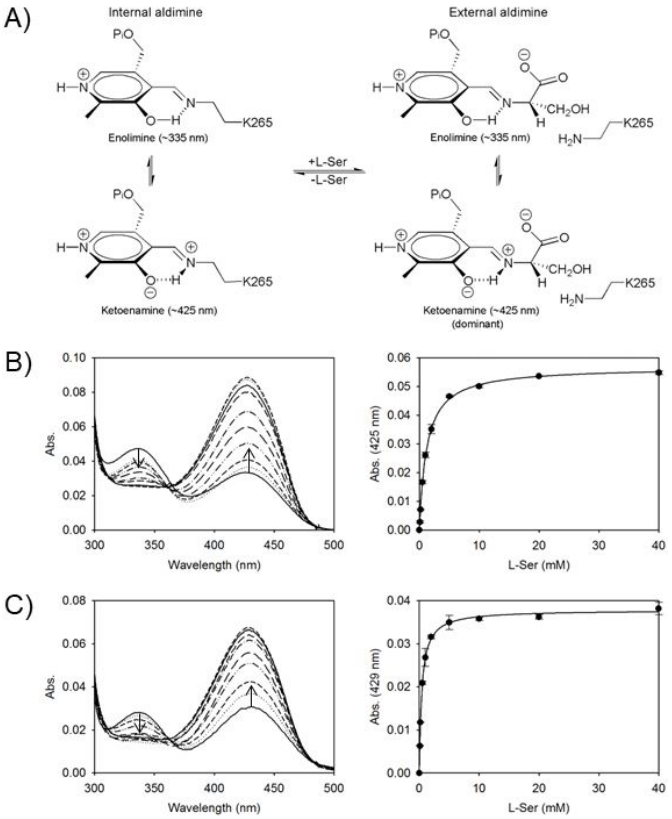

Figure 6. A) Structures of enolimine and ketoenamines in *Sp*SPTase. B) Absorbance spectra for R378K *Sp*SPTase (left) and ΔA^{425} (right) in the presence of varying concentrations of L-Ser. C) Absorbance spectra for R378K / Y73N *Sp*SPTase (left) and ΔA^{429} (right) in the presence of varying concentrations of L-Ser. In all spectra, the solid line was obtained from the *holo*-forms in the absence of L-Ser and the dotted and dashed lines were obtained with increasing concentrations of L-Ser (0.1, 0.2, 0.5, 1, 2, 5, 10, 20, and 40 mM). Error bars are standard deviaions derived from triplicate measurements.

In addition, the enolimine / ketoenamine tautomeric equilibrium was notably shifted toward the ketoenamine in the R378 / Y73N double mutant, suggesting a more polar environment. These results clearly showed that Asn at position 73 alters the active site microenvironment, which would affect interactions with PLP and the PLP : L-Ser external aldimine. The 3-fold decrease in the K_D value for L-Ser in the R378K / Y73N double mutant also supports the hypothesis (Table 1).

Steady-state kinetic parameters for the R378K / Y73N *Sp*SPTase double mutant are listed in Table 1, and a comparison of k_{cat} values for the double mutant, wild-type and R378K single mutant *Sp*SPTases are shown in Figure 7. The R378K / Y73N double mutant had an expanded substrate range with activities (0.24-0.44 s^{-1}) that encompassed shorter acyl-CoAs (*n*-C_6-CoA to *n*-C_8-CoA), substrates for which wild-type and R378K *Sp*SPTases are barely active. Furthermore, the double mutant accepted functionalized short chain acyl-CoA substrates as shown in Figure 8. Despite having little effect on k_{cat} values for long acyl-CoAs (*n*-C_{14}-CoA and *n*-C_{16}-CoA, Figure 7), the Y73N substitution dramatically decreased the K_M values for smaller acyl-CoAs (*n*-C_{10}-CoA to *n*-C_{16}-CoA; up to 40-fold lower) as well as the K_M value for L-Ser as compared to the previously reported value for the R378K *Sp*SPTase (7-fold lower).[24]

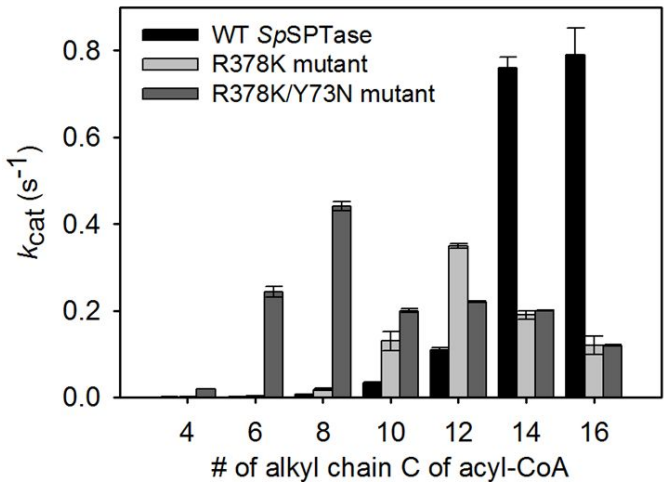

Figure 7. **Comparison of turnover numbers for the R378K / Y73N *Sp*SPTase mutant with the wild-type and parent R378K enzymes.** Because of low activities for shorter chain acyl-CoAs (*n*-C_4-CoA to *n*-C_8-CoA), activities of the wild-type, R378K and R378K / Y73N *Sp*SPTases were determined in the presence of 5 mM substrates (for the R378K / Y73N variant, this was only required for *n*-C_4-CoA).

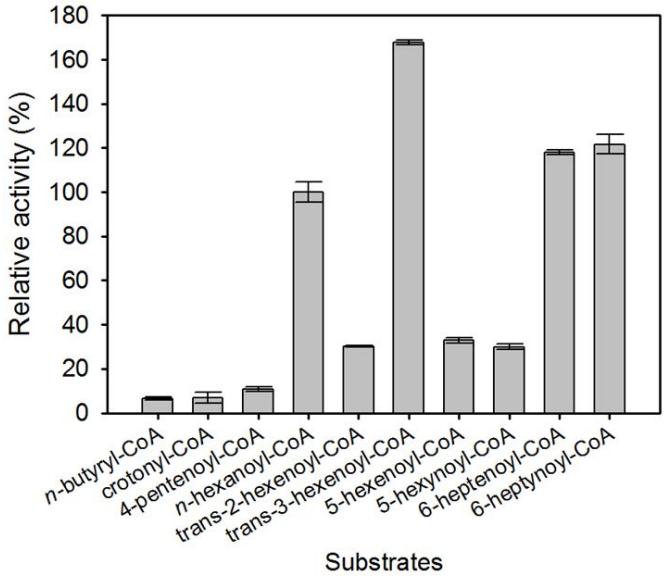

Figure 8. **Relative activities of R378K / Y73N *Sp*SPTase for functionalized acyl-CoAs.**

To investigate the synthetic utility of the best double mutant, we synthesized the KDS analog 3-keto-C_{10}-dihydrosphingosine **1** from L-Ser and *n*-C_8-CoA (Figure 9). Product instability is an issue in these reactions since the desired α-amino-ketone product dimerizes to form 2,5-dihydropyrazine **2** under neutral to alkaline conditions, and this dimer can be irreversibly oxidized to pyrazine **3** by O_2 or H_2O_2.[53, 54] To avoid the latter problem, we carried out the reaction under Ar. Both the rate of dimerization and the equilibrium position between the desired α-amino-ketone monomer **1** and the unwanted 2,5-dihydropyrazine **2** are strongly affected by pH,[55] and the dimer could be hydrolyzed to **1** under acidic conditions.[56] The target was therefore isolated by incubating the product mixture under acidic conditions followed by solvent extraction. The purified product was obtained as a racemic mixture whose measured optical rotation was zero. To determine whether this reflected a lack of stereoselectivity by the enzyme or post-synthesis spontaneous racemization, **1** was incubated under both acidic and neutral conditions in deuterated buffer. The compound showed rapid exchange of the C_α-H peak at neutral pH, but not under acidic conditions (Figure S8). It therefore appears likely that racemization occurred during synthesis. It may be possible to engineer an *Sp*SPTase variant for activity under acidic conditions. Another possibility might be to couple the *Sp*SPTase reaction product with a stereoselective ketoreductase. The rapid racemization of the *Sp*SPTase product should allow for a dynamic kinetic resolution.[57]

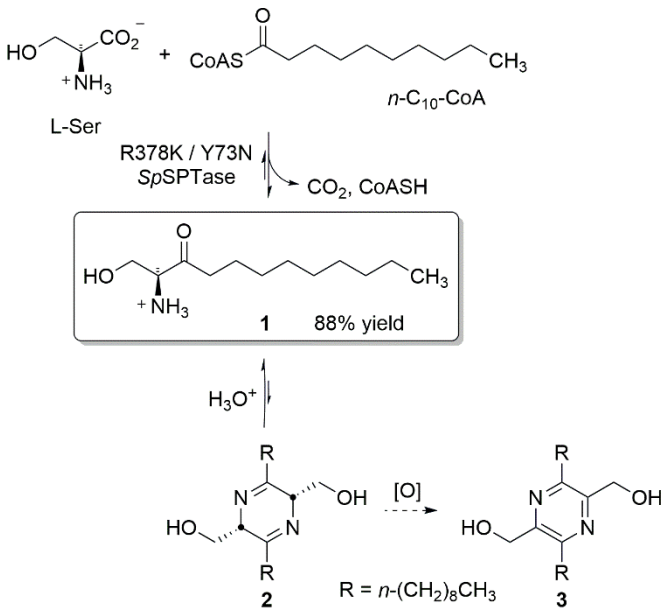

Figure 9. **Synthesis of short-chain KDS analog 1.**

Experimental

Materials

Enzymes for cloning and protein molecular weight standards were purchased from New England Biolabs. Wizard PCR Clean-Up kits were purchased from Promega. Primers were obtained from IDT (Integrated DNA Technologies) and Ellman's reagent, L-Ser, and PLP were purchased from ACROS Organics™. Pantethine was purchased from Jarrow Formulas, Inc. Acid anhydrides were purchased from TCI. Phusion® Hot Start II High-Fidelity DNA polymerase and charcoal decolorizing agent (S25245) were purchased from Fisher Scientific.

ARTICLE

Table 1. Steady-state kinetic parameters for R378K / Y73N SpSPTase with various chain length acyl-CoAs. Error bars reflect differences between duplicate measurements.

Substrate	k_{cat} (s^{-1})	$K_{M,acyl\text{-}CoA}$ (μM)	$K_{M,L\text{-}Ser}$ (mM)	k_{cat} / $K_{M,acyl\text{-}CoA}$ ($M^{-1}s^{-1}$)	$K_{D,L\text{-}Ser}$ (mM)
n-C_4-CoA	*0.020 ± 0.0002*	*7,400 ± 30*		*2.7*	
n-C_6-CoA	*0.24±0.01*	*7,800± 500*		*31*	
n-C_8-CoA	*0.44±0.01*	*730 ± 40*		*600*	
n-C_{10}-CoA	*0.20±0.004*	*85 ± 4*	*0.84±0.03[a]*	*2,400*	*0.43 ± 0.1*
n-C_{12}-CoA	*0.22±0.002*	*150 ± 2*		*1,500*	
n-C_{14}-CoA	*0.20±0.001*	*39 ± 0.4*		*5,100*	
n-C_{16}-CoA	*0.12±0.001*	*2.4 ± 0.1*		*50,000*	

[a]$K_{M,L\text{-}Ser}$ was obtained using n-C_8-CoA

Cloning and NNK Saturation Mutagenesis

A sequence optimized, wild-type *Sp*SPTase gene was synthesized by Genscript (Figure S1), cloned into pET-22b (+) and designated plasmid pHC9.[24] The R378K mutation was incorporated into pHC9 by site-directed mutagenesis using forward (TG AAT ATG GCC AAACCA CCT GCA ACT CCT GCA GGA ACC) and reverse (GT TGC AGG TGG TTT GGC CAT ATT CAC GTA TAA TCC TCC) primers. The resulting plasmid (pHC9-R378K) was used as a template for generating all the double mutant libraries. Site saturation mutagenesis was performed with degenerate primer mixtures (Table S1) using an NNK mixture at the randomized codon (N = A, C, G or T and K = G or T). Each PCR reaction (total volume 100 µL) containing 5 × Phusion HF Buffer (20 µL), pHC9-R378K template (5 ng), forward and reverse primers (0.5 µM each), dNTPs (200 µM each), and DNA polymerase (2 U) was subjected to an initial denaturation step of 98°C (30 s) followed by 18 cycles of 98°C (10 s), 62°C (30 s), and 72°C (210 s). The final extension was performed at 72°C for 300 s. The amplification product was purified with a PCR clean-up kit, eluted with 30 µL nuclease-free water, and treated with *Dpn*I (20 U) overnight at 37°C. The nuclease was inactivated at 80°C for 20 min, then the DNA was purified again using the same kit, eluting with 30 µL of nuclease-free water. The purified DNA (2-3 µL) was used to transform *E. coli* ElectroTen-Blue competent cells (50 µL) by electroporation at a voltage of 2.5 kV (E = 12.5 kV/cm). Immediately after electroporation, 0.4 mL of warm SOC medium was added and cells were incubated at 37°C for 1 h prior to spreading onto LB agar plates containing ampicillin (50 µg/mL). Plates were incubated at 37°C for 14-16 h, then colonies were collected from the plates and combined for pooled plasmid DNA isolation. The pool was used to transform *E. coli* BL21-Gold (DE3) cells (50 µL) by electroporation as described above. After incubating for 1 h in SOC media at 37°C, 10-20 µL aliquots were spread on agar plates containing ampicillin (50 µg/mL) for preparing mutant libraries. Another aliquot (100 µL) was added to 5 mL of LB medium containing ampicillin (100 µg/mL). After shaking overnight at 37°C and 200 rpm, plasmid DNA was isolated from the pooled cells. The library quality (Q_{pool} value) was assessed by Sanger sequencing as previously reported,[25] and the values are shown in Table S1. Primers used for site-directed mutagenesis at the Tyr 73 position are in listed in Table S2.

Chemical Synthesis of Acyl-CoAs

Coenzyme A disulfide dimer (CoA-S-S-CoA) was synthesized from pantethine using three His-tag-purified *E. coli* enzymes (pantetheine kinase, UniProt P0A6I3; phosphopantetheine adenyltransferase, UniProt P0A6I6; dephospho-coenzyme A kinase, UniProt P0A6I9) in the presence of ATP, then free CoASH was prepared by adding TCEP (1 equiv.) at room temperature.[27] Acyl-CoAs were synthesized using CoASH and the corresponding acid anhydrides at 25-35°C using literature methods.[28-30] The successful synthesis of *n*-acyl-CoAs was verified by HPLC, and their concentrations were calculated using A^{260} values (free CoASH, ε^{260} = 16,400 $M^{-1}\cdot cm^{-1}$).[31]

HPLC Methods

All acyl-CoAs (*n*-C_4-CoA to *n*-C_{16}-CoA) were analyzed by reversed-phase HPLC using a 150 × 4.6 mm Synergi Hydro-RP80 Å column with KH_2PO_4 (25 mM) and acetonitrile (100%) employed as solvents A and B, respectively, at a flow rate of 1 mL/min. Initial conditions (0.6% solvent B) were maintained prior to the analysis. After sample injection, a linear increase to

3.6% solvent B over 0.5 min was immediately followed by a linear increase to 5.6% solvent B over 1.5 min, then a linear increase to 17.8% solvent B over 2 min and 80% solvent B over 2 min. After a 5 min hold at 80% solvent B, a linear decrease to 0.6% solvent B over 1 min was followed by a 2 min hold at the initial conditions (0.6% solvent B). The A^{260} value of the eluant was monitored.

Autoinduction and Screening Method

One microliter aliquots of overnight-cultured cells in LB medium supplemented with 100 µg/mL ampicillin were transferred to individual deep wells of a 96-well plate containing ZYM-5022 autoinduction medium (1 mL per well) supplemented with ampicillin (100 µg/mL) as previously described.[24] The plate was incubated at 30°C and 350 rpm for 20 h. Cells were harvested by centrifuging at 2,600 × *g* and the supernatant was discarded. To each well was added 50 µL lysis buffer (50 mM KP_i, pH 7.5, 150 mM NaCl) containing 0.2 mM PLP. The cells were lysed by three cycles of freezing for 90 min at -80°C and thawing for 90 min at 37°C. The last freezing step was performed overnight. An additional 950 µL of lysis buffer was added to each well after the final thawing step, then the cell debris was pelleted by centrifuging at 2,600 × *g* for 30 min at 4°C. Enzyme activity screening assays were carried out in a 96-well plate by adding 10 µL of the cell lysate to 190 µL of reaction buffer (500 mM KP_i, pH 7.5, 150 mM NaCl, 20 mM L-Ser, 1 mM EDTA, 10 µM PLP, 1 mM *n*-C_8-CoA and 0.3 mM Ellman's reagent). The plate was incubated at 37°C and A^{412} was monitored for 5 h. Error bars represent differences between duplicate measurements.

Enzyme Activity Assays

The overexpression, purification and activity assays of *Sp*SPTase mutants using Ellman's reagent were performed as described previously.[24] Specific activities were determined using His-tag-purified proteins (1.5 - 2.7 µM) and 1 mM *n*-acyl-CoAs (C_4-C_8). Reactions were followed by monitoring A^{412} and error bars represent differences between duplicate measurements. Kinetic assays were performed by adding purified R378K / Y73N *Sp*SPTase (0.14-6.4 µM) to a reaction mixture (100 mM KP_i, pH 7.5, 150 mM NaCl, 50 mM L-Ser, 10 µM PLP and 0.2 mM Ellman's reagent) containing *n*-acyl-CoAs at 25°C. Various concentrations of *n*-acyl-CoA substrates were used (1.0-5.0 mM *n*-C_4-CoA, 0.75-5.0 mM *n*-C_6-CoA, 0.25-3.0 mM *n*-C_8-CoA, 0.050-0.6 mM *n*-C_{10}-CoA, 0.050-0.6 mM *n*-C_{12}-CoA, 0.010-0.30 mM *n*-C_{14}-CoA, and 0.005-0.040 mM *n*-C_{16}-CoA). Lineweaver-Burk plots are shown in Figure S2.

UV-Vis Spectral Analysis

UV-Vis spectra were recorded at room temperature in buffer (20 mM KP_i, 150 mM NaCl,10 µM PLP, pH 7.5) containing *Sp*SPTase (10 µM) after pre-incubating the mixture for 30 min. Changes in A^{425} or A^{429} were plotted against the concentration of L-Ser and fitted to a hyperbolic saturation equation:

$$\Delta A_{\mathrm{obs}} = \frac{\Delta A_{\mathrm{max}} \cdot [\text{L-Ser}]}{K_{\mathrm{D,L-Ser}} + [\text{L-Ser}]}$$

where ΔA_{obs} and ΔA_{max} represent the observed and maximal absorbance change at 425 nm (or 429 nm), [L-Ser] is the concentration of L-serine, and $K_{\mathrm{D,L\text{-}Ser}}$ is the dissociation constant for L-Ser.

Relative Activities with Functionalized Substrates

Functionalized acyl-CoAs were synthesized by the W416G mutant of AMP-forming acetyl-CoA synthetase (EC 6.2.1.1) from *Methanothermobacter thermautotrophicus* (MT-ACS1).[32, 33] The *N*-terminally His-tagged protein was heterologously expressed in *E. coli* BL21-Gold (DE3) and purified as reported previously.[34] The enzyme (final concentration 0.6 µM) was added to a reaction mixture containing 100 mM KPi, 150 mM NaCl, pH 7.5, 50 mM L-Ser, 2 mM CoASH, 10 mM MgATP and 20 mM of the desired carboxylic acid. The reaction was performed at 65°C until completion (as determined by measuring the residual free CoASH using Ellman's reagent). After removal of insoluble Mg_2PP_i by centrifugation, the supernatant was used directly for *Sp*SPTase reactions. To the acyl-CoA solution (175 µL) was added EDTA (30 mM), PLP (10 µM), Ellman's reagent (0.2 mM), and R378K / Y73N *Sp*SPTase (2.9 µM) with a final reaction volume of 0.2 mL. Enzyme activity with *n*-C_6-CoA was set to 100% and error bars represent differences between duplicate measurements.

Production of 3-Keto-C_{10}-dihydrosphingosine from L-Ser and n-*C_8-CoA by R378K / Y73N* Sp*SPTase*

Purified R378K / Y73N *Sp*SPTase (2 mg) was added to 20 mL of reaction buffer (50 mM KP_i, 150 mM NaCl, 20 mM L-Ser, 10 µM PLP, 2 mM *n*-C_8-CoA, pH 7.5). The mixture was incubated without stirring under Ar overnight at room temperature, then extracted with $CHCl_3$ (3 × 20 mL). The organic layers were added to a round bottom flask containing 10 mL of Ar-purged 0.1 M HCl and the mixture was vigorously stirred for 5 min, then the organic solvent was evaporated under reduced pressure at 35°C and the aqueous solution was stirred overnight at room temperature under Ar. Water was removed under reduced pressure, then the residue was dissolved in 10 : 1 $CHCl_3$: MeOH and filtered through silica to remove salts. After evaporating the solvent under reduced pressure, the desired product was obtained as solid (7.9 mg, 88%). The product structure was confirmed by NMR spectroscopy (Figure S3) and MS analysis (Figure S4). ^{1}H NMR (300 MHz, CD_3OD) δ 0.90 (t, *J*=6.8 Hz, 3 H) 1.23 - 1.40 (m, 8 H) 1.63 (quin, *J* =7.0 Hz, 2 H) 2.64 (t, *J* =7.3 Hz, 2 H) 3.98 (dd, *J* =12.2, 3.4 Hz, 1 H) 4.10 (dd, *J*=12.0, 4.2 Hz, 1 H) 4.18 (t, *J* =3.8 Hz, 1 H) ppm. as appropriate.

Conclusions

Based on its three-dimensional structure, we subjected 20 residues that lined the active site and acyl-CoA substrate binding region of *Sp*SPTase to site-saturation mutagenesis. Surprisingly, changes at only one of these positions (73) altered acyl-CoA substrate binding properties. The improvement benefited from synergistic non-additivity of mutational effects, a phenomenon that has been observed previously and reviewed recently by Hollmann *et al*.[58] Several Tyr 73 variants accepted shorter acyl-CoA substrates and the Asn replacement proved best, with significantly better catalytic activities for shorter acyl-

CoAs (*n*-C_6-CoA to *n*-C_8-CoA). We also used UV-Vis spectroscopy and steady-state kinetics to probe the effect of substituting Tyr 73 with Asn. Our results underscore the importance of position 73 in dictating substrate selectivity as well as in stabilizing the PLP : L-Ser external aldimine during the catalytic cycle of *Sp*SPTase. Moreover, the R378K / Y73N double mutant tolerated both alkenyl- and alkynyl-substituted acyl-CoAs, both of which could provide chemical handles for further synthetic manipulations. These observations, as well as the successful preparation of 3-keto-C_{10}-dihydrosphingosine by the double mutant opens many possibilities for preparing a range of KDS analogs that can in turn serve as building blocks for sphingolipid analogs.

Author Contributions

H.C. and J.D.S. planned the course of the study. H.C. developed the library screening methodology and carried out the bulk of the experimental work, with contributions from M.C. and A.W. H.C. wrote the first draft of the manuscript, which was revised by J.D.S.

Conflicts of interest

There are no conflicts to declare.

Acknowledgements

We gratefully acknowledge financial support by the NSF (CHE-1705918) and the U.F. University Scholar Program (M.C.). The Mass Spectrometry Research and Education Center is supported by NIH (S10 OD021758-01A1).

Notes and references

1. S. L. Heaver, E. L. Johnson and R. E. Ley, *Curr. Opin. Microbiol.*, 2018, **43**, 92-99.
2. J. Ohanian and V. Ohanian, *Cell. Mol. Life Sci.*, 2001, **58**, 2053-2068.
3. J. C. M. Holthuis, T. Pomorski, R. J. Raggers, H. Sprong and G. Van Meer, *Physiol. Rev.*, 2001, **81**, 1689-1723.
4. A. S. B. Olsen and N. J. Faergeman, *Open Biol.*, 2017, **7**, 170069.
5. E. Gulbins, S. Walter, K. A. Becker, R. Halmer, Y. Liu, M. Reichel, M. J. Edwards, C. P. Muller, K. Fassbender and J. Kornhuber, *J. Neurochem.*, 2015, **134**, 183-192.
6. Y. A. Hannun and L. M. Obeid, *Nat. Rev. Mol. Cell Biol.*, 2018, **19**, 673-673.
7. N. Gerlach, M. Mentel, T. Koehler, B. Tuchscherer, B. Garbe, J. Uelker, H. Tronnier, U. Heinrich and M. Farwick, *Clin. Cosmetic Invest. Dermatol.*, 2016, **9**, 191-203.
8. J. Liu, B. S. Beckman and M. Foroozesh, *Future Med. Chem.*, 2013, **5**, 1405-1421.
9. K. Adachi and K. Chiba, *Perspectives Med. Chem.*, 2007, **1**, 11-23.
10. C. R. Strader, C. J. Pearce and N. H. Oberlies, *J. Nat. Prod.*, 2011, **74**, 900-907.
11. R. E. Toman, V. Movsesyan, S. K. Murthy, S. Milstien, S. Spiegel and A. I. Faden, *J. Neurosci. Res.*, 2002, **68**, 323-330.
12. L. Puglielli, B. C. Ellis, A. J. Saunders and D. M. Kovacs, *J. Biol. Chem.*, 2003, **278**, 19777-19783.
13. B. M. Barth, S. J. Gustafson and T. B. Kuhn, *J. Neurosci. Res.*, 2012, **90**, 229-242.
14. N. Karasavvas, R. K. Erukulla, R. Bittman, R. Lockshin and Z. Zakeri, *Eur. J. Biochem.*, 1996, **236**, 729-737.
15. H. Azuma, S. Ijichi, M. Kataoka, A. Masuda, T. Izumi, T. Yoshimoto and T. Tachibana, *Bioorg. Med. Chem.*, 2007, **15**, 2860-2867.
16. A. Ghosh and S. K. Chattopadhyay, *Tetrahedron: Asymmetry*, 2017, **28**, 1139-1143.
17. R. C. So, R. Ndonye, D. P. Izmirian, S. K. Richardson, R. L. Guerrera and A. R. Howell, *J. Org. Chem.*, 2004, **69**, 3233-3235.
18. T. Yamamoto, H. Hasegawa, T. Hakogi and S. Katsumura, *Org. Lett.*, 2006, **8**, 5569-5572.
19. H. Yang and L. S. Liebeskind, *Org. Lett.*, 2007, **9**, 2993-2995.
20. J. M. Lee, H. S. Lim and S. K. Chung, *Tetrahedron: Asymmetry*, 2002, **13**, 343-347.
21. T. Yamamoto, H. Hasegawa, T. Hakogi and S. Katsumura, *Org. Lett.*, 2006, **8**, 5569-5572.
22. M. C. C. Raman, K. A. Johnson, B. A. Yard, J. Lowther, L. G. Carter, J. H. Naismith and D. J. Campopiano, *J. Biol. Chem.*, 2009, **284**, 17328-17339.
23. G. Han, K. Gable, L. Yan, M. J. Allen, W. H. Wilson, P. Moitra, J. M. Harmon and T. M. Dunn, *J. Biol. Chem.*, 2006, **281**, 39935-39942.
24. H. Choe, M. S. Cha and J. D. Stewart, *Enzyme Microb. Technol.*, 2020, **137**, 109515.
25. B. Sullivan, A. Z. Walton and J. D. Stewart, *Enzyme Microb. Technol.*, 2013, **53**, 70-77.
26. G. L. Ellman, *Arch. Biochem. Biophys.*, 1959, **82**, 70-77.
27. L. M. M. Mouterde and J. D. Stewart, *Org. Proc. Res. Develop.*, 2016, **20**, 954-959.
28. P. V. Vignais and I. Zabin, *Biochim. Biophys. Acta*, 1958, **29**, 263-269.
29. P. P. Constantinides and J. M. Steim, *Arch. Biochem. Biophys.*, 1986, **250**, 267-270.
30. E. J. Simon and D. Shemin, *J. Am. Chem. Soc.*, 1953, **75**, 2520-2520.
31. R. Teufel, C. Gantert, M. Voss, W. Eisenreich, W. Haehnel and G. Fuchs, *J. Biol. Chem.*, 2011, **286**, 11021-11034.
32. C. Ingram-Smith, B. I. Woods and K. S. Smith, *Biochemistry*, 2006, **45**, 11482-11490.
33. C. Ingram-Smith and K. S. Smith, *Archaea*, 2007, **2**, 95-107.
34. L. M. M. Mouterde and J. D. Stewart, *Enz. Microb. Technol.*, 2019, **128**, 67-71.
35. J. M. Wadsworth, D. J. Clarke, S. A. McMahon, J. P. Lowther, A. E. Beattie, P. R. R. Landgridge-Smith, H. B. Broughton, T. M. Dunn, J. H. Naismith and D. J. Campopiano, *J. Am. Chem. Soc.*, 2013, **135**, 14276-14285.
36. E. Kuznetsova, M. Proudfoot, S. A. Sanders, J. Reinking, A. Savchenko, C. H. Arrowsmith, A. M. Edwards and A. F. Yakunin, *FEMS Microbiol. Rev.*, 2005, **29**, 263-279.
37. H. Ikushiro, S. Fujii, Y. Shiraiwa and H. Hayashi, *J. Biol. Chem.*, 2008, **283**, 7542-7553.
38. L. Pezzementi, M. Rowland, M. Wolfe and I. Tsigelny, *Invertebrate Neurosci.*, 2006, **6**, 47-55.
39. J. Griffin and P. C. Engel, *Enzyme Res.*, 2010, **2010**, 951472-951472.
40. X. G. Wang and P. C. Engel, *Protein Eng.*, 1994, **7**, 1013-1016.
41. B. A. Yard, L. G. Carter, K. A. Johnson, I. M. Overton, M. Dorward, H. Liu, S. A. McMahon, M. Oke, D. Puech, G. J. Barton, J. H. Naismith and D. J. Campopiano, *J. Mol. Biol.*, 2007, **370**, 870-886.
42. H. C. Dunathan, *Proc. Natl. Acad. Sci. USA*, 1966, **55**, 712-716.
43. A. C. Eliot and J. F. Kirsch, *Ann. Rev. Biochem.*, 2004, **73**, 383-415.
44. M. C. C. Raman, K. A. Johnson, D. J. Clarke, J. H. Naismith and D. J. Campopiano, *Biopolymers*, 2010, **93**, 811-822.

45. S. P. Webster, D. Alexeev, D. J. Compopiano, R. M. Watt, M. Alexeeva, L. Sawyer and R. L. Baxter, *Biochemistry*, 2000, **39**, 516-528.
46. H. Ikushiro, M. M. Islam, A. Okamoto, J. Hoseki, T. Murakawa, S. Fujii, I. Miyahara and H. Hayashi, *J. Biochem.*, 2009, **146**, 549-562.
47. A. Schmidt, J. Sivaraman, Y. Li, R. Larocque, J. A. R. G. Barbosa, C. Smith, A. Matte, J. D. Schrag and M. Cygler, *Biochemistry* 2001, **40**, 5151-5160.
48. I. Astner, J. O. Schulze, J. van den Heuvel, D. Jahn, W.-D. Schubert and D. W. Heinz, *EMBO J.*, 2005, **24**, 3166-3177.
49. H. Ikushiro, A. Nagami, T. Takai, T. Sawai, Y. Shimeno, H. Hori, I. Miyahara, N. Kamiya and T. Yano, *Sci. Rep.*, 2018, **8**, 14228.
50. J. Lowther, G. Charmier, M. C. Raman, H. Ikushiro, H. Hayashi and D. J. Campopiano, *FEBS Lett.*, 2011, **585**, 1729-1734.
51. M. P. Hill, E. C. Carroll, M. C. Vang, T. A. Addington, M. D. Toney and D. S. Larsen, *J. Am. Chem. Soc.*, 2010, **132**, 16953-16961.
52. S. A. Ahmed, P. McPhie and E. W. Miles, *J. Biol. Chem.*, 1996, **271**, 8612-8617.
53. A. Bunke, O. Zerbe, H. Schmid, G. Burmeister, H. P. Merkle and B. Gander, *J. Pharm. Sci.*, 2000, **89**, 1335-1341.
54. G. A. Hunter, E. Rivera and G. C. Ferreira, *Arch. Biochem. Biophys.*, 2005, **437**, 128-137.
55. E. K. Jaffe and J. S. Rajagopalan, *Bioorg. Chem.*, 1990, **18**, 381-394.
56. A. Luedtke, K. Meng and J. W. Timberlake, *Tetrahedron Lett.*, 1987, **28**, 4255-4258.
57. M. Fornarotto, L. Xiao, Y. Hou, K. A. Koch, E. C. Chang, R. M. O'Malley, T. A. Black, M. B. Cable and S. S. Walker, *Biochim. Biophys. Acta*, 2006, **1761**, 52-63.
58. F. Hollmann, J. Sanchis and M.T. Reetz, *Angew. Chem. Int. Ed.* 2024, **63**, e202404880.

Data availability statement

The data supporting this article have been included as part of the Supplementary Information.